

Equalization Enhanced Phase Noise in Coherent Receivers: DSP-Aware Analysis and Shaped Constellations

Aymeric Arnould, Amirhossein Ghazisaeidi

Abstract—We revisit the analysis of equalization-enhanced phase noise (EEPN) arising in coherent receivers from the interaction between the chromatic dispersion compensation by an electronic equalizer and the phase noise of the local oscillator. Through numerical simulations we highlight EEPN characteristics and investigate its impact on the behavior of the carrier phase recovery algorithm. We show that the blind phase search, which is usually used in practice to recover the carrier phase, partially mitigates the EEPN. We detail a numerical approach to predict the system performance including the phase recovery algorithm, and show that taking into account EEPN characteristics relaxes the constraint on the system laser phase noise given by previous pessimistic analytical models. We present experimental validations of our claims, and address future advanced transoceanic systems using 98 Gbd probabilistically shaped QAM formats.

Index Terms—Coherent receivers, carrier phase recovery (CPR), digital signal processing (DSP), equalization-enhanced phase noise (EEPN), optical communication

I. INTRODUCTION

It has been shown that the interaction between the electronic dispersion compensation (EDC) filter and the phase noise of the local oscillator (LO) laser in the coherent receiver generates a noise called equalization enhanced phase noise (EEPN) [1]– [7]. The variance of EEPN at EDC output is computed in [1]. The EEPN-induced constraints on LO linewidth have been experimentally characterized in [2] on quadrature-phase-shift-keying (QPSK) signals, and simulation results in [3] highlighted tighter requirements for higher modulation formats such as 16 and 64QAM.

Assuming that EEPN is an independent additive white Gaussian noise (AWGN), the EEPN variance was added to that of the amplified spontaneous emission (ASE) noise, and the EEPN system penalty was derived in terms of the optical signal to noise ratio (OSNR) in [4]. To limit the impact of EEPN on system design, hardware solutions have been proposed, such as digital coherence enhancement (DCE) technique developed in [5]. It is shown in [6] that the EEPN impairing the QPSK signal can be partially mitigated by the Viterbi-Viterbi phase recovery, so that the previous analytical study overestimates the EEPN impact on system design. The probability density function of EEPN noise is studied in [7].

A. Arnould and A. Ghazisaeidi are with the Nokia Bell Labs, Paris-Saclay, Nozay 91620, France (e-mail: aymeric.arnould@nokia.com). ©2019 IEEE. Personal use of this material is permitted. Permission from IEEE must be obtained for all other uses, in any current or future media, including reprinting/republishing this material for advertising or promotional purposes, creating new collective works, for resale or redistribution to servers or lists, or reuse of any copyrighted component of this work in other works.

In this work, we revisit the EEPN analysis, carrying out a detailed numerical DSP-aware characterization, including the blind phase search (BPS) [8] as the carrier phase recovery (CPR) algorithm, and study the EEPN penalty for emerging probabilistically shaped constellations recently proposed for transoceanic distances [9], [10]. We believe this revision is timely, as the current industry trend is towards ever increasing symbol-rates: 100 Gbd is now practical. And there is also demands for extremely long distance submarine cables, beyond 15000 km. In this context, accurate analysis of EEPN penalty is important. Even if EEPN arises only from the phase noise of the local oscillator laser, we show that taking into account the transmitter laser phase noise is required, since BPS is included in the analysis, and its optimum moving average filter length depends on both transmitter and receiver phase noise, although only the latter results in EEPN. Note that theoretical DSP-aware analysis of EEPN is prohibitively complex, and experimental characterizations require multiple laser sources with widely different linewidths whereas numerical simulation is an efficient approach to this problem. So we adopt numerical simulation as the main analysis tool in this work. We also present some experimental results to complement our studies. More experimental work is required, and will be presented in future works.

This paper is organized as follows. In section II, we introduce the reduced model of coherent optical transmission system used in this work. In section III, the DSP-aware numerical approach used to investigate the EEPN is presented. We also present our available (but not sufficient) experimental characterizations. In section IV, numerical results are provided to quantify constraints on laser linewidth in the presence of EEPN for transoceanic systems with large accumulated chromatic dispersion, high baud-rate and advanced shaped constellations. In section V, the paper is concluded.

II. SYSTEM MODEL

We use the equivalent baseband model described in Fig. 1a. Previous studies [1], [4] have shown that transmitter (TX) laser phase noise impacts only phase recovery but has no influence on EEPN. First, we will omit TX phase noise to characterize EEPN. Then, it will be included in the rest of the study to quantify the impact of EEPN in a realistic system, where phase noise arising from both LO and TX lasers must be considered to evaluate the system performance after DSP.

A train of symbols x_k at the rate $B = 1/T_s$ is passed through the equivalent transfer function $H(f)$ modeling

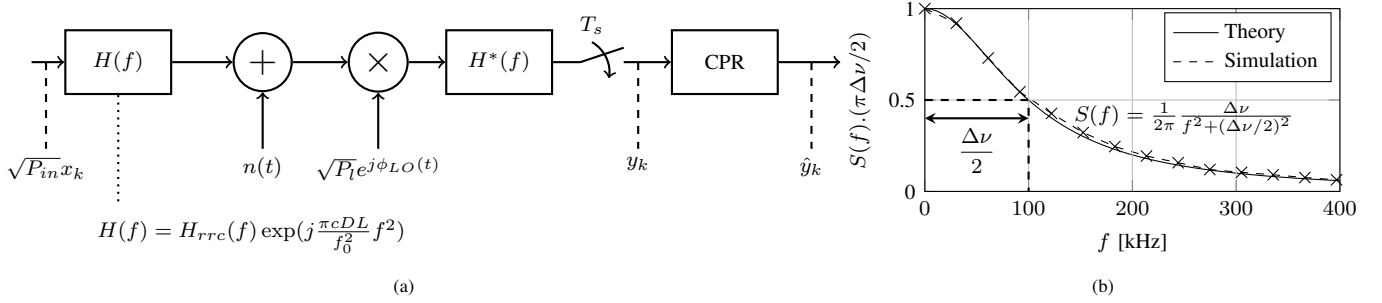


Fig. 1. (a) System baseband model with $H(f)$: channel response, $H_{rrc}(f)$: root raised cosine transfer function, roll-off 0.01, c : the speed of light, D : fiber dispersion coefficient, L : transmission length, f : frequency, f_0 : channel center frequency, $H(0) = \sqrt{T_s}$, T_s : symbol duration, $n(t)$: ASE noise process, $\phi_{LO}(t)$: local oscillator phase noise process, P_{in} : signal mean power, P_l : LO power, CPR: carrier phase recovery, *: complex conjugation; (b) power spectral density $S(f)$ of the power normalized local oscillator field, $\Delta\nu$: laser linewidth.

pulse-shaping and fiber chromatic dispersion. The ASE process $n(t)$ is complex circular and additive white Gaussian noise (AWGN). At the receiver, the signal is multiplied by the local oscillator field. The LO phase noise process $\phi_{LO}(t)$ is a Wiener process; therefore, the continuous-wave optical field of the LO laser has a Lorentzian spectrum with linewidth $\Delta\nu$ (cf. Fig. 1b). The DSP consists of matched filtering (including EDC) modeled by $H^*(f)$, symbol-spaced sampling at the rate B , and the CPR algorithm. The sampled received symbol at CPR input (output) is denoted by y_k (\hat{y}_k).

We denote the EEPN term at CPR input by w_k . It is defined by the following equation

$$y_k = \sqrt{P}x_k e^{j\phi_k} + n_k + w_k, \quad (1)$$

where $\phi_k = \phi_{LO}(kT_s)$ is the sampled LO phase, $n_k = n(kT_s)$ the sampled ASE noise, and $P = \sqrt{2P_l P_{in}}$ the received signal power after coherent mixer.

At the receiver, the CPR gives an estimate $\hat{\phi}_k$ of the carrier phase and rotates the received signal by this estimated phase $\hat{\phi}_k$ such that the signal after CPR is $\hat{y}_k = y_k e^{-j\hat{\phi}_k}$. The total distortion, including ASE, residual phase noise and residual EEPN after CPR, is denoted by N_k and is written as

$$N_k = \hat{y}_k - \sqrt{P}x_k e^{j\phi_k}. \quad (2)$$

Finally, we compute the variance σ_N^2 of the total noise N_k and estimate the signal-to-noise ratio (SNR) of the received signal after CPR as $SNR = P/\sigma_N^2$.

III. DSP-AWARE EEPN CHARACTERIZATION

A. EEPN identification before Carrier Phase Recovery

We performed Monte Carlo simulations and studied statistical properties of the EEPN. We considered a polarized 64QAM channel transmission over EX3000 fiber (dispersion coefficient $D = 20.6$ ps/nm/km) with central frequency $f_0 = 194$ THz and neglected nonlinear impairments. We set $P_{in} = 0$ dBm, $P_l = 10$ dBm, and $OSNR = 20$ dB/0.1nm. We generated 10 sample functions of the LO phase noise process over a time window including 2^{17} symbols, and threw out 15000 symbols from each side of every simulated waveform, to avoid biasing the statistics by the numerical transients. In the simulations, we generated and saved the x_k , ϕ_k and n_k , such that once y_k

was produced, w_k could be extracted without ambiguity using its definition in eq. (1).

For a link of $L = 6600$ km, Fig. 2 compares the analytical variance computed in [1] for a baudrate B of 49 GBd (98 GBd) drawn in solid (dashed) line, and the variance σ_w^2 of the EEPN term w_k computed from the numerical simulations, for 49 GBd (black circles) and 98 GBd (white circles), as functions of the LO linewidth $\Delta\nu$. We show that, before CPR, our simulations and identification of EEPN term as w_k match the analytical model of [1] for the EEPN variance

$$\sigma_{EEP N}^2 = \frac{\pi c D L B \Delta\nu}{2 f_0^2}. \quad (3)$$

Note that (3) is valid for normalized transmitted symbols and therefore, $\sigma_{EEP N}^2$ has been here multiplied by the signal power P to meet our definition of EEPN term, which does not use power normalization.

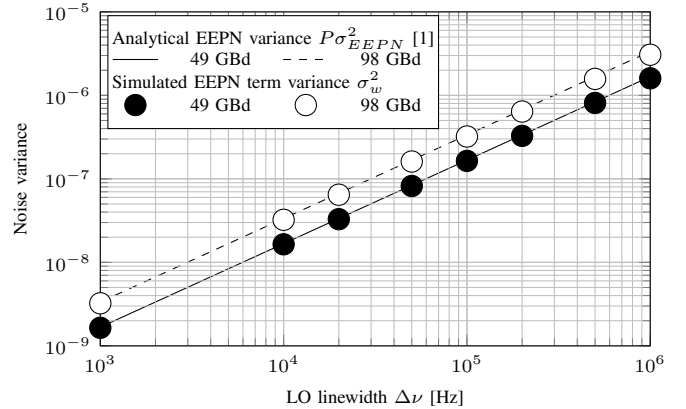


Fig. 2. Analytical and numerical EEPN variance evolution as a function of LO linewidth, for 49 and 98 GBd 64QAM transmission through 6600 km EX3000

Fig. 3a shows the normalized probability distribution function (PDF) of the real part of the EEPN term w_k at CPR input (dashed line), as well as the Gaussian fit (solid line), showing that w_k is not Gaussian. The normalized PDF of the real part of the total noise $n_k + w_k$ is plotted in fig. 3b (dashed line), and fits a Gaussian shape (solid line). Even if the EEPN part can not be considered as a Gaussian noise, the

total noise accounting for ASE and EEPN remains Gaussian in the considered setup.

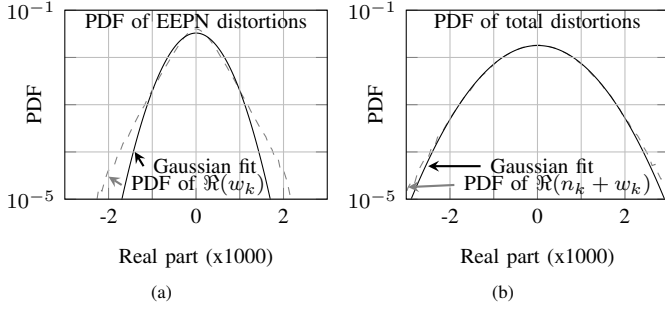


Fig. 3. Probability density function (PDF) of the real part of EEPN distortions at carrier phase recovery (CPR) input w_k (a) and total distortions at carrier phase recovery (CPR) input $n_k + w_k$ (b). Numerical simulations were performed for a 49 GBd 64QAM transmission through 6600 km EX3000, neglecting nonlinearity, with OSNR equal to 20 dB/0.1nm and LO linewidth set to 200 kHz.

For 49 GBd transmission over 6600 or 13419 km, fig. 4 shows the normalized amplitude of the cross-correlation R_n between the EEPN distortions with ideal data remodulation $w_k x_k^*$ and the LO field $e^{j\phi_k}$, defined as

$$R_n = \langle (w_k x_k^*)^* e^{j\phi_{k+n}} \rangle = \langle w_k^* x_k e^{j\phi_{k+n}} \rangle \quad (4)$$

We observe a one-sided width at half maximum of around 400 symbols for 6600 km, and 760 symbols for 13419 km. This shows that the EEPN is a colored noise which depends on link properties and is correlated to the LO phase noise. Therefore, taking into account the influence of the phase recovery DSP in the analysis is a must.

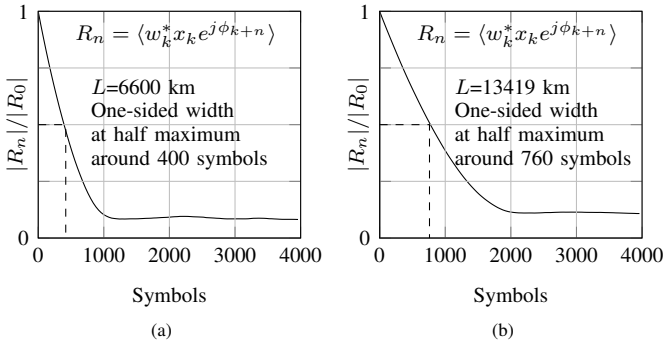
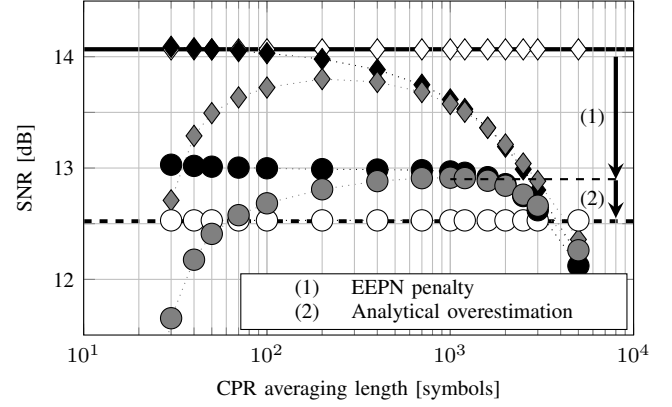


Fig. 4. Signal-EEPn cross-correlation for a 49 GBd 64QAM transmission through (a) 6600 km or (b) 13419 km EX3000, neglecting nonlinearity, with OSNR equal to 20 dB/0.1nm and LO linewidth set to 200 kHz.

B. Carrier Phase Recovery influence

To study the behavior of CPR algorithms in the presence of EEPN, we consider three different cases of CPR implementation to describe the performance of the system. First, we perform a LO phase cancellation, i.e. we assume $\hat{\phi}_k = \phi_k$, which requires a perfect knowledge of the random process ϕ_k . Next, we use ideal data remodulation (IDR), namely, we assume perfect knowledge of the transmitted symbols x_k and compute the estimated phase over an averaging block of length $N = 2l + 1$ as $\hat{\phi}_k = \angle \sum_{k=-l}^l y_k x_k^*$. Finally, to study the



Analytical:
 — ASE only - - - ASE + equivalent AWGN [1]
Simulation with ASE, without EEPN (dispersion kept to 0):
 ◊ LO phase cancellation ◆ IDR ◇ BPS
Simulation with ASE and EEPN:
 ○ LO phase cancellation ● IDR ● BPS

Fig. 5. SNR vs. CPR averaging length, for LO phase cancellation, IDR and BPS carrier phase estimation of a 49 GBd 64QAM transmission through 6600 km EX3000, neglecting nonlinearity, with OSNR equal to 20 dB/0.1nm and LO linewidth set to 200 kHz.

performance of a realistic transmission use-case, in the third case the estimated phase $\hat{\phi}_k$ is computed as the output of the BPS algorithm with an averaging block of length $N = 2l + 1$. Note that when using BPS, in this paper, all cycle slips are removed to avoid performance degradation from ambiguity coming from constellation symmetry.

Assuming the same setup as in fig. 3 and with the three different CPR techniques, we computed the received signal \hat{y}_k after CPR and we plot the estimated SNR in Fig. 5. The solid black line is the theoretical SNR for a fixed OSNR of 20 dB/0.1nm, assuming that ASE is the only source of noise. Next, we turn on LO phase noise but keep dispersion to zero: just as a numerical sanity check, white diamonds corresponding to LO phase cancellation (when ϕ_k is used as $\hat{\phi}_k$) meet the solid line of the theoretical SNR; black diamonds correspond to ideal data remodulation (IDR) whereas gray diamonds show the result of the BPS algorithm over a block of $N = 2l + 1$ symbols. For short CPR averaging, the black diamonds reach the theoretical performance, showing that LO phase noise is completely removed by data remodulation. As the block length increases, the LO phase noise tracking is degraded by the averaging process and the performance decreases. The gray diamonds corresponding to BPS exhibit an optimal averaging length around 200 symbols. Below this optimum, phase estimation is degraded by ASE noise which is not sufficiently averaged by the CPR process. Beyond this optimum, the averaging window is too long and does not allow to follow the LO phase noise, hence the BPS performance curve converges to that of the IDR curve, and both IDR and BPS performance degrade due to not following the phase noise Wiener process.

Next, we turn on the dispersion (hence EEPN): white circles represent the performance with CPR by LO phase cancellation, black circles correspond to the IDR with perfect knowledge of transmitted symbols, and gray circles are the

result of BPS. We observe that the phase recovery by LO phase cancellation meets the case where EEPN is modeled as an equivalent AWGN (dashed line) with the variance computed in [1] and is *not* the best strategy to perform CPR in presence of EEPN. Even if we have perfect knowledge of the LO phase noise, as shown in [6], using LO phase noise as phase estimate $\hat{\phi}_k$ is non-optimal as it ignores that the phase to be removed by the CPR is a combination of LO phase noise ϕ_k , transmitted symbols x_k and CDC equalizer transfer function $H(f)$. Consequently, the black circles representing ideal data remodulation exhibit the best performance among the three considered cases in the presence of EEPN: for short averaging length, it reaches a SNR level which is 0.6 dB greater than that achieved by AWGN equivalent noise model; the performance decreases slowly when the averaging length increases (only 0.2 dB when the block size varies from 30 to 1000), before decreasing strongly when the averaging process does not allow to track the phase variations anymore. Finally, we show that the BPS algorithm (gray circles) exhibits an optimal performance which almost reaches the ideal data remodulation case, outperforming the analytical prediction by 0.4 dB when the averaging block length is set to 1000. In the presence of EEPN, the optimal performance is attained for longer averaging block length compared to phase-noise-only case. This change of behavior of the BPS algorithm in the presence of EEPN can be considered as a signature of EEPN non-white nature, showing that the BPS must be taken into account in the study of EEPN impact. The SNR offset labeled as (1) on Fig. 5, shows the true EEPN penalty with respect to optimized BPS. This penalty could be avoided if an ideal EEPN compensator were available. The SNR offset labeled as (2) is the amount by which the closed form formula, as per (3) overestimates the EEPN penalty.

C. Impact of modulation format choice

Previous analysis was performed assuming 64QAM modulation. Now we study the influence of modulation format on BPS performance in presence of EEPN. Assuming the same setup as the one resulted in the curves of Fig.5, we plot in Fig.6, in presence of EEPN, the SNR after BPS for QPSK (black circles), 64QAM (gray circles) and probabilistically shaped PCS64QAM, with source entropy equal to 5.4 bits/symbol (black diamonds). The theoretical performance with EEPN modeled as equivalent AWGN is drawn in dashed line. Compared to 64QAM, QPSK shows better resilience to CPR averaging length variation, with a stable SNR performance of almost 13 dB with moving average filter lengths varying from 50 to 1000. For the short averaging length where the phase estimation process is limited by the ASE noise, decision errors arise more often with constellations with high cardinality and small distances between symbols. For PCS64QAM, this degradation drastically falls at low averaging lengths, indicating that probabilistically shaped format imposes even tighter constraints on the CPR parameter than the high cardinality unshaped formats. However, the maximum achieved SNR for all the constellations is very similar, provided the moving average length is separately optimized four

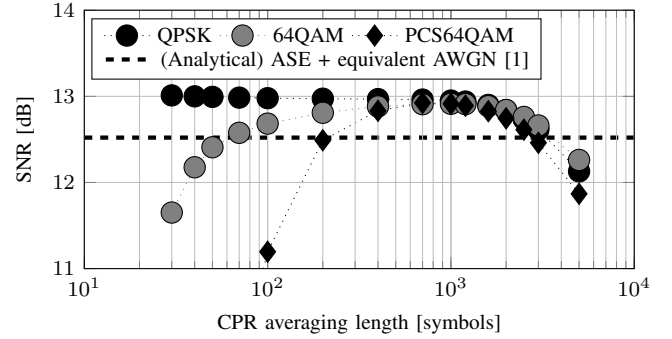


Fig. 6. SNR vs. CPR averaging length, for optimized as BPS carrier phase estimation of a 49 GBd transmission using QPSK, 64QAM or PCS64QAM, through 6600 km EX3000, neglecting nonlinearity, with OSNR equal to 20 dB/0.1nm.

each format. The block averaging length must be optimized in each configuration and under this condition, in this example, the degradation from the advanced formats remains negligible at the optimal point of operation.

To further investigate format dependence of EEPN penalty, in presence of optimized BPS, in Fig. 7 we plot the received SNR versus LO laser linewidth for a 49 GBd and a 98 Gbd transmission using QPSK (black circles), 64QAM (gray circles) and the PCS64QAM (black diamonds), through 6600 km EX3000, neglecting nonlinearity, with OSNR equal to 20 dB/0.1nm. The solid line shows the theoretical performance in the absence of EEPN, whereas the dashed line indicates the analytical performance when EEPN is modeled as an equivalent AWGN using Eq. (3). At low linewidths, all the formats reach the theoretical SNR without EEPN, which differs by 3 dB between 49 and 98 GBd, corresponding only to a doubling of ASE noise in the channel bandwidth. Note that, for all formats, the achieved SNR with BPS is higher than what is analytically predicted with equivalent AWGN. At high linewidths, the excess EEPN penalty PCS64QAM with respect to QPSK is inferior to 0.3 dB at 1 MHz linewidth. The takeaway is that the EEPN penalty is only mildly format dependent. For simplicity, in the rest of the paper, we will only focus on the emerging probabilistic format to study EEPN penalty on long-haul transmission system design, as it represents the worst case.

D. Experimental validation

To assess the impact of EEPN on BPS observed in the simulations, we performed an experimental characterization using a C+L recirculating loop depicted in Fig. 8. The C-band transmitter (TX C) is described in details on the Figure. The test channel is a single tunable laser source (TLS) at wavelength 1545.72 nm modulated with a polarization-multiplexed I/Q (PM I/Q) modulator, surrounded by 2 loading channels, each of which driven by a distinct modulator, and further multiplexed by 86 loading channels modulated by a third dedicated modulator. Each modulator is driven by a digital-to-analogue (DAC) loaded with different randomly-generated sequences operating at 49 GBd. A wavelength selective switch (WSS) and a coupler are used to combine the

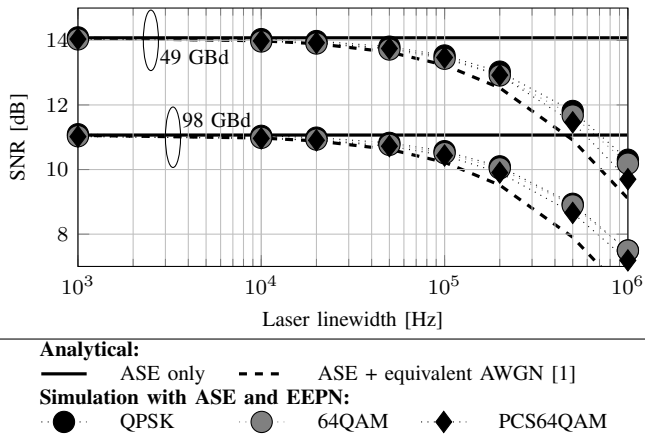


Fig. 7. SNR vs. LO laser linewidth, for optimized BPS as CPR of a 49 GBd or 98 GBd transmission using QPSK, 64QAM or PCS64QAM, through 6600 km EX3000, neglecting nonlinearity, with OSNR equal to 20 dB/0.1nm.

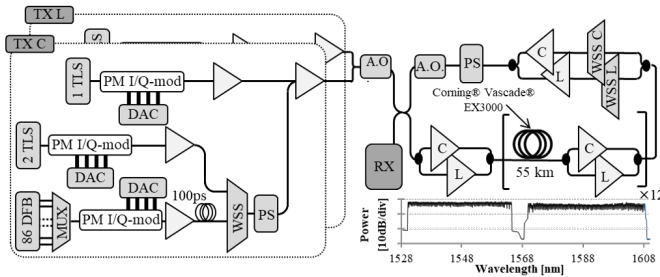


Fig. 8. Experimental setup for experimental WDM 49 GBd PCS64QAM transmission over 6600 km EX3000

measured channel with the loading channels. A fiber spool and a polarization scrambler (PS) ensure de-correlation of the loading channels. This TX C is coupled to a similar L-band transmitter (TX L) before being launched in the recirculating loop. The loop is composed of twelve 55 km spans of EX3000 fiber. The loop includes a gain equalizer WSS per band and a loop synchronous polarization scrambler. After 10 loops, the signal is sent to a coherent receiver and sampled by a real-time scope with 33 GHz bandwidth, working at 80 Gsamples/s.

Fig. 9 shows the SNR vs. BPS averaging length, after DSP including EDC, polarization de-multiplexing with a multi-modulus algorithm (MMA) preceded by pre-convergence by constant modulus algorithm (CMA), carrier frequency estimation and phase recovery using BPS and pilot-based cycle-slip removal using 1% pilots and least-mean square adaptive post-equalization. The dashed lines represent three measured back-to-back SNR vs. filter length curves for OSNRs equal to from 17 dB, 18 dB and 19 dB. The evolution of the SNR in these back-to-back measurements (hence without dispersion) is given as reference for various amount of ASE noise, as both EEPN and fiber nonlinear impairments are absent in back-to-back measurements. Then, we plot in gray circles the performance of the transmission case, after 6600 km EX3000, with a launched power of 16 dBm. This launched power has been chosen, as shown on the bell curve in the inset, to be 2 dB below the nonlinear threshold (NLT) to ensure that the nonlinear distortions are negligible, but EEPN is present. We

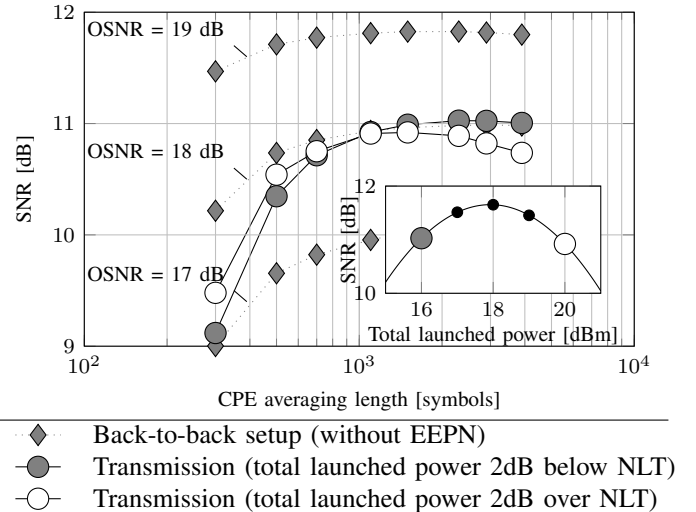


Fig. 9. Experimental SNR vs. BPS averaging length, for a back-to-back configuration (without EEPN) and a WDM 49 GBd PCS64QAM transmission over 6600 km EX3000, for total launched power 2 dB below or over NLT. Inset: SNR vs. total launched power.

observe that at low BPS averaging length the transmission SNR falls more sharply than back-to-back SNR, and that in the transmission case the optimal performance is achieved for longer averaging block size compared to the back-to-back case, as was observed in the numerical simulations of the previous section. We plot in white circles the transmission SNR with launched power of 20 dBm, which corresponds to 2 dB above the NLT. In the presence of fiber nonlinearity, the performance drops for long averaging block size, ensuring that the difference of behavior between the previous transmission case (at 16 dBm) and the back-to-back configuration is not attributable nonlinearities, but the signature of the presence of EEPN. As the BPS behaves differently in the transmission case and in back-to-back case with various ASE variances, this shows that EEPN must not be considered as an equivalent AWGN and the BPS must be taken into account to evaluate system performance.

IV. EEPN IMPACT ON SYSTEM DESIGN

A. OSNR penalty definition

To assess the amount by which system performance could be underestimated due to simplifying assumptions, in Fig. 10 we plot the estimated SNR after digital signal processing vs. OSNR curves, assuming the same numerical setup as in Fig. 3 and sweeping the ASE noise variance. The operative SNR at the considered configuration was set to $SNR_{ref} = 12$ dB according to [9] and the EEPN impact is considered in term of OSNR penalty to reach this operative SNR. The solid line is the theoretical SNR vs. OSNR curve assuming both laser linewidth and dispersion are zero. Next, we turn on LO phase noise but keep dispersion to zero: gray diamonds correspond to BPS, where the averaging length has been optimized to maximize the SNR. The penalty between solid black line and gray diamonds corresponds to the residual noise coming from the use of BPS as CPR and is denoted PN penalty. Next, we turn on dispersion (hence EEPN) and optimize BPS, to obtain gray

circles, which represent the true system performance including EEPN and impact of DSP. Performance degradation from gray diamonds to gray circles is the EEPN penalty, whereas the degradation from black solid line to gray circles represents the total OSNR penalty due to both PN and EEPN, which is about 1 dB for this specific configuration and operative SNR of 12 dB. For low OSNRs the BPS performance without EEPN (diamonds) converges to that of BPS performance with EEPN (circles), showing that in this regime the performance is mainly due ASE and PN, and not EEPN. The dashed line is the analytical performance estimated when EEPN is modeled as an independent AWGN with the variance computed in [1], and shows that ignoring DSP overestimates the EEPN penalty by 0.3 dB in this configuration.

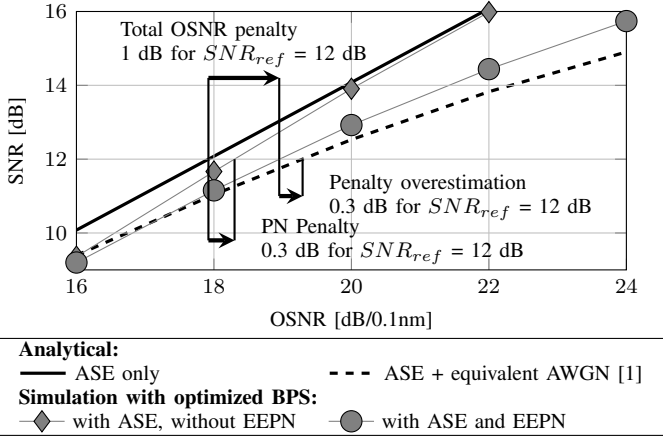


Fig. 10. SNR vs. OSNR (referred to 0.1 nm) of a single-channel single-polarization 49 GBd PCS64QAM through 6600 km EX3000, neglecting nonlinearity, and LO linewidth equal to 200 kHz

B. Impact on modern and future transoceanic systems

For the PCS64QAM transmission over transoceanic links of 6600 or 13419 km, with baud-rates of 49 or 98 GBd, we computed the previously defined PN and total OSNR penalties and we plot in Fig. 11 these penalties vs. laser linewidth. Firstly, we set TX laser linewidth to 0, and only swept the LO linewidth. In this case, white circles stand for total EEPN penalty, whereas white diamonds correspond penalty only due to PN, *i.e.*, we artificially set fiber dispersion coefficient to zero, so the EEPN was also forced to zero. Secondly, we performed simulations where both TX laser source and LO linewidth were swept, but for simplicity assumed these two lasers have the same linewidth. In this case black circles represent the total EEPN penalty, and black diamonds correspond to PN only penalty. For each simulation point, the BPS was separately optimized for maximum SNR. The dashed line represents the DSP-agnostic penalty predicted by the analytical model [1] where EEPN is modeled as an equivalent AWGN. Given this analytical model does not capture the CPR, its predictions do not depend on TX laser linewidth

Fig. 11a presents simulation results for transatlantic transmission of 49 GBd PCS64QAM over 6600 km, with a target SNR of 12 dB (parameters set according to [9]). For low linewidths, EEPN and PN penalties are similar and they are

slightly higher than the analytical prediction, due to BPS implementation penalty. As the linewidth increases, EEPN increasingly dominates PN. When TX laser linewidth is set to zero, for LO linewidths larger than 20 kHz, the total OSNR penalty (white circles) is always lower than the pessimistic analytical prediction. When TX laser linewidth is set to that of LO, even if TX laser phase noise does not directly contribute to EEPN generation, this additional phase noise impacts BPS optimum point. As a result, the PN penalty (black diamonds) and the total penalty (black circles) increase and to keep EEPN penalty under 1 dB of OSNR, we must limit the linewidth at 130 kHz.

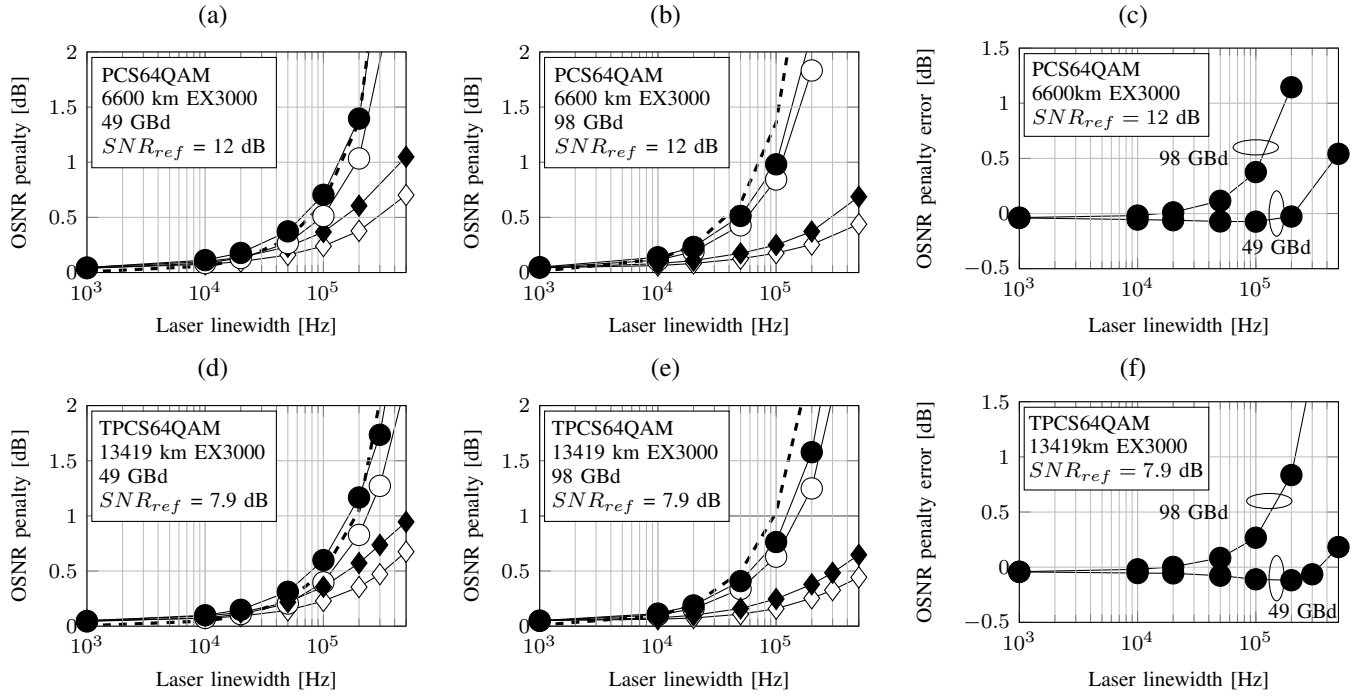
Since the industry trend is towards increasing the per-channel baud rate, hence reducing transponder count and cost-per-bit, on Fig. 11b, we examine the OSNR vs. linewidth penalty of 98 GBd PCS64QAM on the same link as in Fig. 11a. In the analytical model, EEPN variance scales linearly with the baudrate: as a result, OSNR penalty increases as we double the baudrate. To keep EEPN penalty under 1 dB of OSNR, the analytical model gives a linewidth constraint on LO and TX of 70 kHz. When TX linewidth is set to 0, the total OSNR penalty is smaller than the analytical model. Besides, increasing the baudrate reduces the share of PN penalty in the total OSNR penalty. As a result, when both TX and LO linewidths are nonzero, the linewidth constraint on both lasers to keep OSNR penalty under 1 dB is loosened to 100 kHz.

Then, we plot the OSNR penalty discrepancy between the analytical model and our DSP-aware simulations in Fig. 11c for the case where TX laser linewidth equals LO linewidth. At 49 GBd, the analytical model overestimates by 0.5 dB the OSNR penalty at 500 kHz linewidth. At 98 GBd, the PN penalty is reduced.

As the EEPN penalty scales up with total transmission distance, we also studied a transpacific transmission of TPCS64QAM over 13419 km EX3000. In order to meet transmission experiment parameters from [10], the target SNR is set to 7.9 dB, hence both EEPN and ASE increase. In Fig. 11d, we show simulation results from 49 GBd transmission. The PN penalty (white diamonds:TX source linewidth set to zero, black diamonds: TX laser linewidth equal to LO linewidth) is comparable to that of 6600 km transmission of Fig. 11a. To keep EEPN penalty under 1 dB of OSNR, we must limit TX and laser to 150 kHz.

The 98 GBd transpacific results are plotted in Fig. 11d. In order to keep EEPN OSNR penalty under 1 dB, the TX and LO linewidth should be kept below 120 kHz.

Finally, we plot OSNR penalty discrepancy between the analytical model and our simulations in Fig. 11e. For 49 GBd transmission, the overestimation by the analytical model remains under 0.3 dB for both LO and TX linewidths smaller than 500 kHz. However, for 98 GBd transmission, we observe more than 1 dB penalty overestimation for linewidth over 220 kHz when both TX and LO generate phase noise. Please note that the revised assessment of EEPN, is not only useful for setting requirements on laser specifications, but also to separate the extra penalty due to EEPN from other sources of penalty in advanced characterizations of submarine systems, which require an accuracy of less than 0.1 dB on SNR.


Analytical:

- - - ASE + equivalent AWGN [1], [4]

Simulation with ASE and EEPN, phase noise generated by LO only:

○ Total OSNR penalty ◇ PN penalty (no dispersion)

Simulation with ASE and EEPN, phase noise generated by LO and TX:

● Total OSNR penalty ◆ PN penalty (no dispersion)

Fig. 11. Simulation results of OSNR penalty induced by EEPN as a function of LO linewidth for a single-channel transmission through EX3000 fiber, neglecting nonlinearity. For a transatlantic 6600 km with PCS64QAM transmission, OSNR penalty is given for 49 GBd (a) and 98 GBd (b), and OSNR penalty error between simulations and analytical model is shown in (c). For a transpacific 13419 km with TPCS64QAM transmission, (c) and (d) show OSNR penalty for 49 GBd and 98 GBd, and (e) gives the OSNR penalty error between simulations and analytical model.

V. CONCLUSIONS

We characterized the electronically enhanced phase noise (EEP) in coherent receivers, taking into account the blind phase search algorithm. We showed the influence of EEP on the behavior of this carrier phase recovery process, and quantified EEP penalty as a function of local oscillator linewidth for emerging transoceanic systems with shaped constellations, highlighting the importance of DSP-aware performance analysis. Not taking into account the EEP characteristics and the BPS effect on OSNR penalty can lead to overestimate its impact on system design. As both TX and LO play a role in the CPR algorithm, even if TX does not generate EEP, both of them must be included in the simulations to estimate the full PN impact, which accounts for BPS residual error and EEP. For high baudrate transmission, EEP penalty becomes dominant and the overestimation is significant for current laser source performance. These penalty curves might serve as guidelines for specifications of the laser sources for high baudrate coherent systems in future.

REFERENCES

- [1] W. Shieh and K. Ho, "Equalization-enhanced phase noise for coherent-detection systems using electronic digital signal processing," *Opt. Express*, 16(20), pp. 15718-15727 (2008).
- [2] C. Xie, "Local Oscillator Phase Noise Induced Penalties in Optical Coherent Detection Systems Using Electronic Chromatic Dispersion Compensation," *Optical Fiber Communication Conference and National Fiber Optic Engineers Conference*, Optical Society of America, 2009, p. OMT4.
- [3] I. Fatadin and S. J. Savory, "Impact of phase to amplitude noise conversion in coherent optical systems with digital dispersion compensation," *Opt. Express*, 18(15), 16273-16278 (2010)
- [4] A. Kakkar, J. R. Navarro, R. Schatz, H. Louchet, X. Pang, O. Ozolins, G. Jacobsen, and S. Popov, "Comprehensive Study of Equalization-Enhanced Phase Noise in Coherent Optical Systems," *Journal of Lightwave Technology*, 33(23), pp. 4834-4841 (2015).
- [5] G. Colavolpe, T. Foggi, E. Forestieri, and M. Secondini, "Impact of Phase Noise and Compensation Techniques in Coherent Optical Systems," *Journal of Lightwave Technology*, 29(18), pp. 2790-2800 (2011)
- [6] R. Farhodi, A. Ghazisaeidi, and L. A. Rusch, "Performance of carrier phase recovery for electronically dispersion compensated coherent systems," *Opt. Express*, 20(24), pp. 26568-26582, (2012).
- [7] R. Farhodi, A. Ghazisaeidi, and L. A. Rusch, "Analytical PDF of Decision Statistic for Coherent MPSK with Electronic Dispersion Equalization," *National Fiber Optic Engineers Conference*, Optical Society of America, 2012, p. JW2A.56.
- [8] T. Pfau, S. Hoffmann, and R. Noé, "Hardware-Efficient Coherent Digital Receiver Concept With Feedforward Carrier Recovery for M -QAM Constellations," *Journal of Lightwave Technology*, 27(8), pp. 989-999 (2009).
- [9] A. Ghazisaeidi, I. F. de Jauregui Ruiz, R. Rios-Müller, L. Schmalen, P. Tran, P. Brindel, A. Carbo Meseguer, Q. Hu, F. Buchali, G. Charlet, and J. Renaudier, "Advanced C+L-Band Transoceanic Transmission Systems Based on Probabilistically Shaped PDM-64QAM," *Journal of Lightwave Technology*, 35(7), pp. 1291-1299 (2017).
- [10] O. Ait Sab, A. Ghazisaeidi, P. Plantady, A. Calsat, I. F. de Jauregui Ruiz, S. Dubost, P. Pecci, J. Renaudier, and V. Letellier, "376 Pb/sxkm Transmission Record over 13,419km Using TPCS-64QAM and C-Band

EDFA-Only,” *Asia Communications and Photonics Conference*, Optical Society of America, 2017. p. Su2B.2.